Environmental Pollution 376 (2025) 126408

Contents lists available at ScienceDirect

Environmental Pollution

journal homepage: www.elsevier.com/locate/envpol

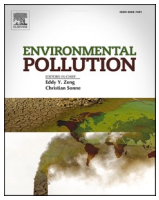

Investigating aquatic biodegradation and changes in the properties of pristine and UV-irradiated microplastics from conventional and biodegradable agricultural plastics☆

Ula Putar [a], Aida Fazlić [b], Lukas Brunnbauer [c], Janja Novak [a], Anita Jemec Kokalj [a,d], Jernej Imperl [a], Jiří Kučerík [e], Petra Procházková [b], Stefania Federici [f], Rachel Hurley [g], Andrijana Sever Škapin [h,i], Pavlína Modlitbová [b], Pavel Pořízka [b,j], Jozef Kaiser [b,j], Andreas Limbeck [c], Gabriela Kalčíková [a,j,*]

[a] Faculty of Chemistry and Chemical Technology, University of Ljubljana, Večna pot 113, 1000, Ljubljana, Slovenia
[b] Central European Institute of Technology, Brno University of Technology, Purkyňova 656/123, 61200, Brno, Czech Republic
[c] TU Wien, Institute of Chemical Technologies and Analytics, Getreidemarkt 9/164-I^{2}AC, 1060, Vienna, Austria
[d] University of Ljubljana, Biotechnical Faculty, Department of Biology, Jamnikarjeva 101, 1000, Ljubljana, Slovenia
[e] Department of Agrochemistry, Soil Science, Microbiology and Plant Nutrition, Faculty of AgriSciences, Mendel University in Brno, Zemědělská 1752, 613 00, Brno, Czech Republic
[f] Department of Mechanical and Industrial Engineering, University of Brescia & INSTM RU of Brescia, Via Branze 38, 25123, Brescia, Italy
[g] Norwegian Institute for Water Research, Økernveien 94, 0579, Oslo, Norway
[h] Slovenian National Building and Civil Engineering Institute, Dimičeva ulica 12, 1000, Ljubljana, Slovenia
[i] Faculty of Polymer Technology—FTPO, Ozare 19, 2380, Slovenj Gradec, Slovenia
[j] Faculty of Mechanical Engineering, Brno University of Technology, Technická 2896/2, 61669, Brno, Czech Republic

ARTICLE INFO

Keywords:
Biodegradability
Aging
Aquatic ecosystem
Degradation
Microplastics
Mulching films

ABSTRACT

There is an increasing tendency to replace conventional agricultural plastic mulching films with biodegradable alternatives. However, while the latter biodegrade well under controlled conditions (e.g. industrial compost), their biodegradation in non-target environments (e.g. aquatic environments) is questioned and poorly understood. Therefore, in this study, microplastics derived from conventional polyethylene (PE) and biodegradable polybutylene adipate terephthalate starch blend (PBAT) mulching films were exposed to UV irradiation and subsequently tested for their ready biodegradability in an aqueous medium where changes in their characteristics were evaluated. The results showed limited biodegradation for pristine and UV-aged PE: no morphological, surface chemical or internal changes were observed. Pristine PBAT showed signs of initial biodegradation, while UV-aged PBAT biodegraded by up to 57%. New functional groups appeared on the PBAT surface after UV irradiation according to FTIR analysis and crystallinity increased after biodegradation. Elemental analysis revealed a range of metals in PE and PBAT microplastics. No changes in metal distribution analysed in microplastic after UV-aging or biodegradation were found, except that less titanium was present in PBAT after biodegradation indicating potential leaching. None of the PBAT microplastics had ecotoxic effects towards the aquatic plant *Lemna minor*. Pristine and UV-aged PE showed negative effects on roots, but these were not observed after biodegradation. Low biodegradation of pristine PBAT and possible leaching of metals demonstrated here raise questions about the sustainable use of biodegradable alternatives, especially when they enter non-target environments.

☆ This paper has been recommended for acceptance by Dr Hocheol Song.

* Corresponding author. Faculty of Chemistry and Chemical Technology, University of Ljubljana, Večna pot 113, 1000, Ljubljana, Slovenia.
E-mail address: gabriela.kalcikova@fkkt.uni-lj.si (G. Kalčíková).

https://doi.org/10.1016/j.envpol.2025.126408
Received 18 February 2025; Received in revised form 7 May 2025; Accepted 8 May 2025
Available online 8 May 2025

1. Introduction

The production and use of plastics have increased dramatically in recent decades due to their versatility and economic feasibility (PlasticsEurope, 2024). However, this widespread use has come at a significant cost to the environment through extensive pollution of aquatic and terrestrial ecosystems (Ghaffar et al., 2022; Napper and Thompson, 2023; Simul Bhuyan et al., 2021) leading to urgent action to mitigate plastic pollution, with an increasing focus on the development of biodegradable alternatives (Dilshad et al., 2021; Moshood et al., 2022; Rosenboom et al., 2022).

In sectors with high plastic consumption, such as agriculture, the transition from conventional plastic to biodegradable is a crucial step in reducing plastic pollution. Unlike conventional plastics, biodegradable alternatives are supposed to be degraded within the soil environment, eliminating the need to collect them after use and minimising agricultural waste. So, the synthesis and production of biodegradable plastics is coupled with testing of their biodegradability in the soil environment (Briassoulis and Dejean, 2010; Chen et al., 2024). Many studies have shown that biodegradable plastics may degrade in soil but the degree and rate of this degradation is affected by the composition of the plastics, presence of additives, and the conditions of the surrounding environment such as soil properties, microbial activity, water content, temperature, and also pre-exposure to the UV irradiation (Afshar et al., 2024; Hoshino et al., 2001; Lambert and Wagner, 2017; Liao and Chen, 2021; Mazzon et al., 2022; Oberlintner et al., 2021; Pischedda et al., 2019). A recent study revealed that polybutylene adipate terephthalate mulching film degrades *in situ* in agricultural soil, but after 16 months of burial in soil, the film degradation was still not complete (approximately 66% of the film degraded) and considerable amount of macro- and microplastics was found in soil (Convertino et al., 2024). Field tests to track the degradation of biodegradable plastics in soil have revealed that the time periods for degradation observed in laboratory tests (to obtain the certification of biodegradation in soil) are indeed also observed under field conditions, but only if *thermal days* and not *calendar days* are taken into account (e.g. Griffin-LaHue et al. (2022)). This highlights an important factor when translating laboratory tests to the field context, where there is a likelihood for biodegradable plastic residues to remain in the soil for several years after use and/or incorporation into soils.

Despite extensive research on the biodegradation of plastic alternatives used in the soil environment, there are concerns about their fate once they enter the aquatic environment (Kaing et al., 2024). This is because biodegradable mulching films can fragment due to UV exposure during agricultural use (Convertino et al., 2024; Yang et al., 2022), and the resulting microplastics can be potentially transferred into water bodies (Ren et al., 2021; van Grinsven and Schubert, 2023). Evidence for the propagation of microplastics from soil environments across wider spatial scales and to connected environments has already been observed (Crossman et al., 2020; Han et al., 2022), demonstrating the potential likelihood for biodegradable plastic fragments to be transferred from terrestrial to aquatic environments. This pathway raises critical questions about the actual biodegradability of these newly synthesised materials in aquatic environments, whose dynamics and consequences differ significantly from those in terrestrial environments.

In this context, the aim of this study was to compare and evaluate the biodegradation of two materials used as mulching films in agriculture — conventional polyethylene (PE) and biodegradable polybutylene adipate terephthalate starch blend (PBAT) — in the aquatic environment (i.e. in ready biodegradability test based on the OECD guidelines (OECD, 1992)) by using different analytical techniques. To increase environmental relevance, the materials were tested both in their pristine form and after exposure to UV irradiation as UV light is one of the most common abiotic degradation factors in the environment (Li et al., 2023). Traditionally, the biodegradability of plastics is evaluated by measurement of oxygen consumption or evolved CO_2 (Pires et al., 2022). However, these methods provide limited insight into the degradation process, and therefore, we coupled a conventional biodegradability test with several analytical techniques to better understand the initial steps of microplastic biodegradation process. The evaluation focused on i) biodegradability in the aquatic environment by measuring oxygen consumption, ii) morphological changes evaluated with scanning electron microscopy (SEM), iii) surface chemical alterations evaluated by Fourier transform infrared spectroscopy (FTIR) and Raman spectroscopy, iv) changes in elemental composition evaluated by laser-ablation inductively coupled plasma mass spectrometry (LA-ICP-MS), v) determination of internal structure modifications by determining crystallinity (by using differential scanning calorimeter (DSC)), and vi) the changes in ecotoxicity with model organism aquatic plant *Lemna minor*. Understanding biodegradation in non-target environments (e.g. aquatic ones) is crucial to fully assess the impact on the environment and effectively communicate about sustainable practices.

2. Material and methods

2.1. Characteristics of microplastics

Microplastics were derived from one conventional PE mulch film (internal code M-PEDE-45-black-A0; P6) and one mulch film made of starch and PBAT (internal code M-BIOEL-15-black-A0, P5) within the EU Horizon project PAPILLONS. Both were black and prepared by cryomilling of the virgin mulching films. Extensive properties of the source material mulching films used for the generation of microplastics and their properties were reported by Hurley et al. (2024). The median size of PE and PBAT were 57 ± 38 μm and 147 ± 44 μm, respectively, and they were irregularly shaped fragments (Jemec Kokalj et al., 2024). Organic and inorganic additives were identified in PE and PBAT – these include a series of light stabilisers and antioxidants to slow the degradation of the material, anti-slip agents used for the production of films, and plasticisers to deliver the properties of the mulching film materials (Hurley et al., 2024).

A portion of the prepared microplastics was subjected to UV–VIS irradiation to simulate accelerated natural weathering. The samples were carefully placed in glass Petri dishes and shielded by a layer of quartz glass to prevent contamination or possible sample loss during exposure. They were exposed in a Q-SUN Xe-3 UV chamber (Q-Lab, Bolton, UK) for accelerated weathering for 10 days (240 h). The chamber was equipped with three 1800 W Xe lamps calibrated to emit wavelengths corresponding to natural sunlight – xenon arc lamps produce the realistic reproduction of full-spectrum sunlight, including ultraviolet, visible light, and infrared radiation. The samples were irradiated with a power of 40 W/m^2 at a chamber temperature of 38 °C and 50% of relative humidity, while the black standard was maintained at a temperature of 50 °C. Throughout the exposure period, the samples were thoroughly mixed and homogenised daily to ensure uniformity and consistency of the aging process. The aged microplastics were labelled as UV-PE and UV-PBAT. The number of simulated days was calculated based on the UV intensity used during aging (40 W/m^2), duration (240 h) and the mean UV-irradiance in Europe (i.e. 60 kWh/(m^2/year) (Gewert et al., 2018),) according to Equation (1) (Chen et al., 2023):

$$\text{Simulated days} = \frac{\text{Total irradiance expose}\,(0.04\,\text{kW/m}^2 \cdot 240\,\text{h})}{\text{Mean UV irradiance in Europe}\,(60\,\text{kW h/(m}^2\text{/year)})} \cdot 365 \quad (1)$$

The number of calculated simulated days was 58, which can be related to the number of days when mulching films are exposed during the seasonal agricultural activity.

2.2. Biodegradability in the aquatic environment

In order to comprehensively evaluate the biodegradability of PE, UV-PE, PBAT, and UV-PBAT, two experimental set-ups, i.e., open and closed

systems, were used. Both systems were operated under comparable conditions (temperature, stirring, content of nutrients and microorganisms, availability of oxygen, time etc.), as required by the OECD ready biodegradability test (OECD, 1992). Details are given in Sections 2.2.1 and 2.2.2. Microplastics from the open system were then analysed using advanced analytical techniques (Section 2.3) to assess the changes due to biodegradation. The closed system was set up to monitor biodegradation as a function of oxygen consumption used for the degradation of microplastics by microorganisms as it is common way how to test aerobic biodegradation of polymeric substances (ISO, 2019). A similar approach using open and closed system was successfully applied in our previous study on tire wear particles (Klun et al., 2023).

2.2.1. Open system

Artificial freshwater with a low concentration of nutrients and microorganisms (50 mg/L activated sludge) (ISO, 2019) was prepared and 200 mL were added to glass bottles, then 200 mg of microplastics (PE, UV-PE, PBAT or UV-PBAT) were added separately to each bottle to reach the final concentration of 1000 mg/L. A blank sample containing only artificial freshwater without the addition of microplastics was also prepared. Two independent replicates of each treatment were performed. The bottles were then placed on a magnetic stirrer, covered with aluminium foil to protect them from light and incubated at 20 ± 2 °C for 28 days. After the test, microplastics (labelled as PE-BIO, PBAT-BIO, UV-PE-BIO, UV-PBAT-BIO) were recovered by filtration (cellulose filters, pore size 7–12 μm, Macherey-Nagel, Germany), both replicates were combined together and analysed using the methods described in Section 2.3.

2.2.2. Closed system

The biodegradability test was also performed in a closed system to assess the degradation of the tested microplastics based on oxygen consumption (ISO, 2019). The test was performed at same time and under comparable conditions as the test in open system, with some minor modifications to meet the requirements of the standard procedure (ISO, 2019). Briefly, the same artificial freshwater was used, and 365 mL was filled into the dark glass bottles. The concentration of microplastics was 100 mg/L, as required by the ISO standard, and microplastic particles (PE, UV-PE, PBAT or UV-PBAT) were added separately to each bottle. In addition, a blank treatment was included, and according to the standard procedure another treatment was prepared to follow the biodegradation of a reference compound (100 mg/L microcrystalline cellulose, Sigma-Aldrich, USA). Three independent replicates of each treatment were performed. Each bottle was then equipped by rubber cap with KOH and sealed with the OxiTop® head (WTW, Germany). The bottles were then placed on a magnetic stirrer in a climate chamber (20 ± 2 °C, dark) and oxygen consumption was measured for 28 days. The degree of biodegradation was calculated according to the standard procedure (ISO, 2019).

2.3. Advanced analytical techniques

Changes in the surface morphology were evaluated using field-emission scanning electron microscopy (FE-SEM) (Section 2.3.1) and surface chemical changes by Attenuated Total Reflectance Fourier-transform infrared spectroscopy (ATR-FTIR) and Raman spectroscopy (Section 2.3.2). The changes in the elemental composition were studied by laser-ablation inductively coupled plasma mass spectrometry (LA-ICP-MS) and prior to LA-ICP-MS, elemental content in each sample was also analysed by conventional digestion followed by liquid ICP-MS (Section 2.3.3). Differential scanning calorimeter (DSC) was used for evaluation of changes in internal structure (i.e., crystallinity) of microplastics (Section 2.3.4).

2.3.1. Surface morphology

The surface morphology and shape of microplastics were evaluated by FE-SEM Zeiss ULTRA plus (Zeiss, Germany) at an accelerating voltage of 2.00 kV. Prior to the FE-SEM analysis, the samples were coated with a thin Au/Pd layer.

2.3.2. Surface chemical changes

To identify surface chemical changes, a FTIR spectrometer (Spectrum Two FT-IR spectrometer, PerkinElmer, USA) with a Universal ATR module was used. The wavenumber ranged from 4000 cm^{-1} to 450 cm^{-1}, with a resolution of 2 cm^{-1} (10 co-scans). Five repetitions for each sample were recorded and averaged. Background and ATR correction of the spectra were applied.

The microplastics were also investigated using Raman spectroscopy. The samples were first fixed onto adhesive tape. For the analysis, a confocal Witec Alpha 300R system (WITec, Germany) was used. The laser employed had a wavelength of 532 nm and operated at a power of 0.5 mW. The integration time for each measurement was set to 1 s. We performed 20 accumulations and collected 10 spectra per sample, then calculated the mean values for spectral analysis. The objective lens used had a 50x magnification. Additionally, an 1800 g/mm grating was utilized.

2.3.3. Changes in the elemental composition

For LA-ICP-MS analysis, individual samples were mounted in acrylic resin (ClaroCit Kit, Struers, Austria) to investigate the lateral distribution of elements. Cross-sections of these embedded samples were prepared by manual sanding using abrasive paper down to a grain size of 5 μm, and then LA-ICP-MS imaging experiments were carried out similarly as described in previous work (Brunnbauer et al., 2024; Pořízka et al., 2023). LA-ICP-MS analysis was carried out using an imageGEO193 laser ablation system (ESL, USA) operating at a wavelength of 193 nm and equipped with a TwoVol3 ablation chamber. Prior to the analysis, a preablation step was applied to remove potential surface contamination from the sample preparation process.

The LA system was coupled to an NexION5000 system (PerkinElmer, USA) using the analytical cup with Tygon® tubing with an inner diameter of 1.6 mm. Samples were ablated under a constant stream of helium (0.8 L/min). Argon was used as a make-up gas (0.86 L/min) and mixed with the sample aerosol using a dual concentric injector (DCI) (ESL, USA) right before the ICP. Kinetic energy discrimination (KED) mode (He) was used to avoid the influence of polyatomic interferences on the measurement. ICP-MS data was recorded using Syngistix 3.5 and LA-ICP-MS data evaluation was carried out using Iolite 4.5.7.1. Data were normalised to 13C to compensate for instrumental drifts. Additional measurement parameters are provided in Table S1.

Prior to LA-ICP-MS, elemental content in each sample was also analysed by conventional digestion followed by liquid ICP-MS. Briefly, samples were accurately weighed into PTFE vessels (with an approximate mass of 75 mg). Then 4 mL of concentrated HNO_3 (67% *(w/w)*, suprapur, Carlo Erba, Italy) and 1 mL of concentrated H_2O_2 (30% *(w/w)*, pro analysi, Fluka, Honeywell, USA) were added. Acid digestion was performed in a microwave system (Ethos UP, Milestone, Italy) with a three-step temperature program: samples were heated to 210 °C (approx. 7.5 °C/min), the set temperature was maintained for 20 min, and then the samples were allowed to cool down to room temperature. Samples were digested in duplicate. The digested solutions were quantitatively transferred to 20 mL volumetric flasks and diluted to the mark with ultrapure water (resistivity >18.2 MΩ/cm, Synergy Water Purification System, Merck Millipore, Germany). Sample solutions were stored in 50 mL polypropylene centrifuge tubes (Sarstedt, Germany). The blank sample was prepared by the same procedure. For the liquid ICP-MS analysis, samples were diluted by a factor of 10 using 1% HNO_3. Additionally, 1 μg/L Indium was added as an internal standard. Liquid ICP-MS analysis was carried out using an iCAP Q TQ ICP-MS (ThermoFisher Scientific, Germany) in KED mode (additional measurement parameters are provided in Table S2). The instrument was tuned daily for the maximum ^{115}In signal while keeping $^{140}Ce^{16}O/^{140}Ce$ below 1.9 %

using Tune A solution (ThermoFisher Scientific, Germany). Metal content for ^{27}Al, ^{56}Fe, ^{39}K, ^{24}Mg, ^{23}Na, ^{60}Ni, ^{208}Pb, ^{47}Ti, ^{68}Zn was determined using a calibration based on a multielement standard (Multi VIII, Certipur®, Merck, Darmstadt, Germany) and a single element standard for Titanium (Certipur®, Merck, Darmstadt, Germany).

2.3.4. Changes in internal structure

DSC (DSC 5500 equipped with an RCS 90 cooling system, TA Instruments, USA) was used to determine the melting enthalpy of polymers, which is proportional to their crystallinity. The device was calibrated using the melting enthalpy and melting temperature of water, indium, tin, and lead. The samples were placed into an aluminum pan (Tzero), weighed, and the pan was hermetically sealed to prevent moisture evaporation. This is crucial because moisture evaporation would produce an endothermic peak that could overlap with the melting endotherm, thereby negatively influencing data analysis. The following protocol was applied: heating from 30 °C to 80 °C at a rate of 10 °C per minute, isotherm for 2 min, heating from 80 °C to 180 °C at 10 °C per minute, cooling from 180 °C to 0 °C at 10 °C per minute, and reheating from 0 °C to 180 °C at 10 °C per minute. The measurements were conducted under a nitrogen flow, with samples being measured at least three times. For the determination of melting enthalpy, the second heating run was used, ensuring the thermal history of the polymer was identical for all samples. The melting enthalpy was determined by integrating the peak area. The obtained energy in Joules, along with the known melting enthalpy of a hypothetical fully crystalline polymer (i.e., 100% crystallinity), was used to determine the crystallinity of measured polymers. Specifically, the melting enthalpy for fully crystalline LDPE is reported as 293 J/g (Niu et al., 2016), and for PBAT, it is 114 J/g (Liu et al., 2022).

2.4. Ecotoxicity

The duckweed *Lemna minor* was selected for an assessment of the ecotoxicity, as it had previously been used for this purpose for microplastics (Boots et al., 2023; Kalčíková et al., 2017; Mateos-Cárdenas et al., 2019; Rozman et al., 2021). The procedure followed the OECD standard method (OECD, 2006). Briefly, 50 mL of Steinberg medium was poured into a 100 mL beaker and 100 mg/L of each type of microplastics was added (PE, UV-PE, PE-BIO, UV-PE-BIO, PBAT, UV-PBAT, PBAT-BIO, and UV-PBAT-BIO). The concentration of microplastics was chosen based on the OECD recommendation (OECD, 2019) and it is also the maximum concentration that is usually used when initially testing the effects of microplastics on aquatic organisms (Jemec Kokalj et al., 2018; Rozman et al., 2022; Rozman and Kalčíková, 2022; Rozman et al., 2021; Zong et al., 2021). A blank sample without microplastics was also prepared. Then 10 fronds of duckweed *Lemna minor* with previously removed roots were placed on the water surface. Each treatment was replicated at least four times. The beakers were incubated for seven days in a climate chamber at 25 ± 1 °C and a light/dark scheme of 16/8 h. After incubation, the inhibition of specific growth rate, root length, and chlorophyll content were assessed according to Rozman et al. (2022).

2.5. Statistical analysis

The normality and homogeneity of variances were tested with the Shapiro-Wilk test and Levene's test, respectively. Differences in biodegradability between PE and UV-PE and between PBAT and UV-PBAT were tested with two-sample *t*-test. Statistically significant differences in crystallinity between different treatments were evaluated by one-way ANOVA, followed by the Tukey test. Data for the toxicity testing were not normally distributed, therefore, the Kruskal-Wallis test, followed by the Dunn's test were used for comparisons between treatments (PE, UV-PE, PE-BIO, UV-PE-BIO, PBAT, UV-PBAT, PBAT-BIO, and UV-PBAT-BIO). All analyses were performed using OriginPro 2023b software (OriginLab Corp., USA) and differences were considered significant if $p < 0.05$.

3. Results

3.1. Biodegradability testing

The biodegradability of pristine (PE, PBAT) and UV-aged (UV-PE, UV-PBAT) microplastics was investigated in a closed system (Fig. 1). The reference compound (microcrystalline cellulose) degraded well under the test conditions confirming the suitability of the test set-up. Both PE and UV-PE showed minimal degradation up to 3%. In the case of PBAT, the maximal biodegradation was up to 15%, but the UV-aging resulted in increased biodegradation up to 57% (the statistically significant difference was visible after day 19, Table S3).

3.2. Morphological changes

The FE-SEM images of pristine PE, UV-PE, and PE-BIO (Fig. 2) showed a comparable smooth surface with some irregularities, while the surface of UV-PE-BIO was more structured, which may be related to the attachment of other particulates and microorganisms of the activated sludge (marked with red arrows). In the case of PBAT, the images of the surface of PBAT and UV-PBAT were comparable, while the morphology of PBAT-BIO and UV-PBAT-BIO changed. The surface of PBAT-BIO was smoother compared to PBAT, while UV-PBAT-BIO also had small holes on the surface.

3.3. Surface chemical changes

The surface chemical composition of the microplastics was investigated using ATR-FTIR and Raman spectroscopy. The FTIR spectra of PE, UV-PE, PE-BIO, and UV-PE-BIO are presented in Fig. 3A and PBAT, UV-PBAT, PBAT-BIO, and UV-PBAT-BIO in Fig. 3B. The main characteristic FTIR bands for PE were clearly visible in all recorded spectra (Fig. 3A). They can be assigned as very intense and sharp peaks of CH_2 asymmetric and symmetric stretching around 2915 and 2850 cm^{-1}, intense peak (doublet, due to crystallinity) of CH_2 bending around 1473 and 1463 cm^{-1}, weak deformation modes of CH_2 and CH_3 around 1370-1350 cm^{-1}, and medium split CH_2 rocking mode peak at 730 cm^{-1} and 720 cm^{-1} (Krimm et al., 1956). According to the FTIR spectra, none of the treatments altered the chemical identity of PE. FTIR spectra of PBAT, UV-PBAT, PBAT-BIO, and UV-PBAT-BIO also showed the main characteristic bands assigned to PBAT polymer (Fig. 3B). The absorption band in the region 3000-2800 cm^{-1} can be ascribed to the C-H stretching region, the very intense and sharp band originating in the region

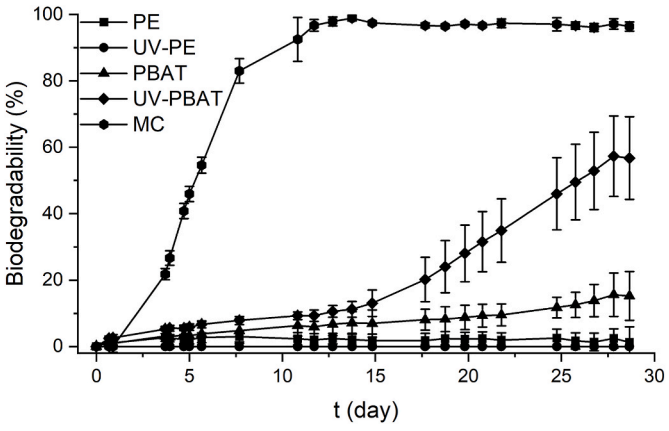

Fig. 1. Biodegradation of a reference compound (microcrystalline cellulose (MC)), pristine (PE and PBAT) and UV pre-treated microplastics (UV-PE and UV-PBAT) in a closed system. Mean values and standard deviations are shown.

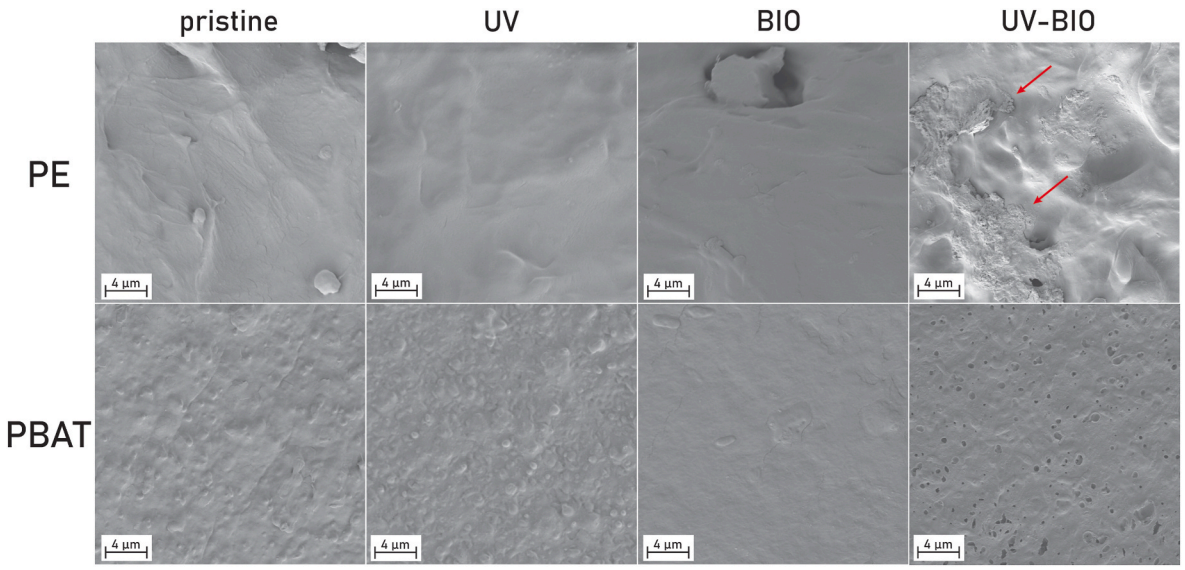

Fig. 2. FE-SEM images of pristine microplastics (PE, PBAT), UV-aged microplastics (UV-PE, UV-PBAT) and microplastics after biodegradation (PE-BIO, PBAT-BIO, UV-PE-BIO, UV-PBAT-BIO). Attached activated sludge biomass is marked with red arrows. (For interpretation of the references to colour in this figure legend, the reader is referred to the Web version of this article.)

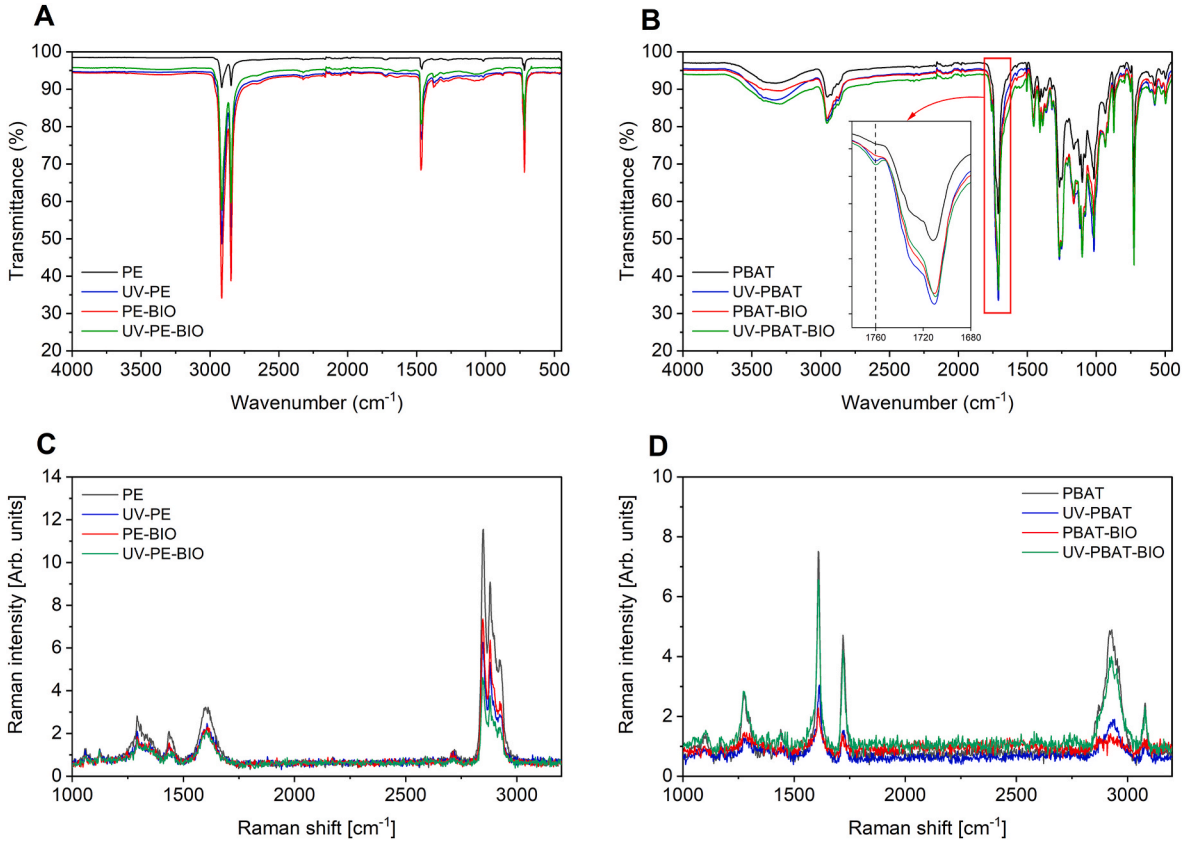

Fig. 3. Results from FTIR analysis for (A) PE and (B) PBAT and Raman spectroscopy for (C) PE and (D) PBAT.

1750-1680 cm^{-1} can be assigned to the stretching vibration adsorption of the carbonyl group in the ester (C=O stretching of ester groups), the region 1270-1000 cm^{-1} can be assigned to the C-O stretching of ester groups, and around 720 cm^{-1} a sharp band can be possibly ascribed to the bending vibration adsorption of CH-plane of the benzene ring (Cai et al., 2013). The inserted graph showed the carbonyl region, highlighting the appearance of a weak peak around 1760 cm^{-1} after UV treatment (UV-PBAT and UV-PBAT-BIO), possibly described as modifications occurring in the ester groups of PBAT due to the treatment. No other significant changes are recorded after the treatments.

Raman spectra of PE, UV-PE, PE-BIO, and UV-PE-BIO and PBAT, UV-PBAT, PBAT-BIO, and UV-PBAT-BIO, are presented in Fig. 3C and D, respectively. The prominent PE peaks in the Raman spectra were observed as bands due to stretching frequencies of C-H bonds around

3000 cm^{-1}, bending and twisting frequencies of C-H bonds at 1300 and 1400 cm^{-1}, and C-C bond stretching between 1000 and 1200 cm^{-1} (Fig. 3C) (PhysicsOpenLab, 2022). Prisitine PE showed the highest peak around 3000 cm^{-1}, followed by PE-BIO, then UV-aged PE and finally the combination of UV and biotic aging. On the other hand, the prominent peaks for PBAT were observed in the Raman spectra at 2927, 1719 and 1090 cm^{-1} (Fig. 3D). These peaks can be attributed to CH_2 and CH_3 vibrations, C=C and C=O stretching, O-CH_2 bending modes, =C-H in the benzene ring and out-of-plane = C-H bending modes (de Souza et al., 2022). The peak at 2927 cm^{-1} was the highest in the pristine sample, followed by the combination of biotic and UV-aging (UV-PBAT-BIO), with the lowest signal observed for PBAT-BIO. From the PCA analysis, it is clear that Raman spectroscopy was able to distinguish not only between different types of microplastics, but also between different types of aging (Fig. S1).

3.4. Changes in elemental composition

LA-ICP-MS analysis was performed to reveal changes in composition for selected metals based on liquid ICP-MS analysis of PE and PBAT (Table S4) after UV aging or/and biodegradation. Liquid ICP-MS revealed the presence of the analysed elements (^{27}Al, ^{56}Fe, ^{39}K, ^{24}Mg, ^{23}Na, ^{60}Ni, ^{208}Pb, ^{47}Ti, ^{68}Zn) in a concentration ranging from close to detection limits to a few hundred μg/g. LA-ICP-MS results showed that all metals analysed were comparable in all PE treatments (Figs. S2–S10), apart from Fe as it accumulated around the PE particles (Fig. S3). In the case of PBAT, the results showed no difference between the metals analysed in the different treatments (Figs. S11–S17), with exception of Ti (Fig. 4). Less Ti was present in microplastics indicating potential leaching out of the PBAT after the biodegradability test. Interestingly, PBAT contained Pb, but it was stable in the polymer matrix and was not leached out during UV irradiation or after the biodegradation test (Fig. 4).

3.5. Changes in internal structure

The changes in the internal structure were evaluated by comparing the crystallinity of the investigated microplastics (Table 1). The crystallinity of PE, UV-PE, PE-BIO, and UV-PE-BIO was comparable (no statistically significant differences between the treatments, Table S5), therefore, none of the treatments changed the internal structure of PE. The changes in crystallinity of pristine PBAT were not statistically significant after UV irradiation ($p = 0.5037$). However, crystallinity was significantly increased after biodegradation, as there were statistically significant differences between PBAT and PBAT-BIO ($p < 0.0001$) and

Table 1
Crystallinity of investigated pristine microplastics (PE, PBAT), after UV exposure (UV-PE, UV-PBAT), and after biodegradation (PE-BIO, PBAT-BIO, UV-PE-BIO, UV-PBAT-BIO) (n = 3, mean ± SD).

Sample	Crystallinity (%)	Sample	Crystallinity (%)
PE	27.4 ± 0.8	PBAT*	16.8 ± 1.7
UV-PE	28.5 ± 0.1	UV-PBAT#	10.4 ± 0.5
PE-BIO	29.1 ± 1.1	PBAT-BIO*	59.4 ± 2.3
UV-PE-BIO	29.4 ± 0.7	UV-PBAT-BIO#	37.0 ± 14.6

* and # - statistically significant difference between PBAT and PBAT-BIO and between UV-PBAT and UV-PBAT-BIO, respectively (Table S5).

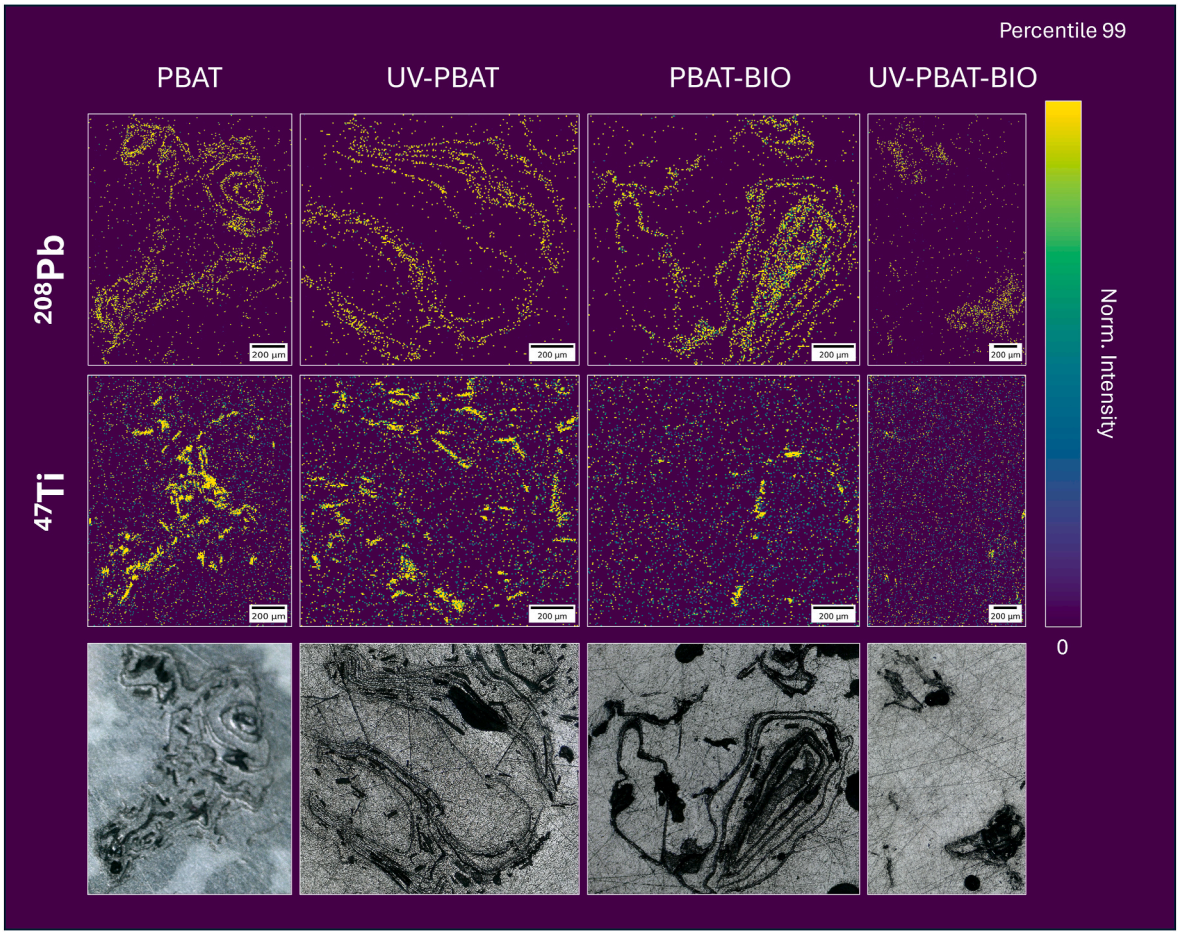

Fig. 4. LA-ICP-MS analysis of Ti and Pb in pristine PBAT, UV pre-treated (UV-PBAT) and after biodegradation (PBAT-BIO, UV-PBAT-BIO).

between UV-PBAT and UV-PBAT-BIO ($p = 0.0029$).

3.6. Changes in ecotoxicity

The results of the ecotoxicity tests showed that there were no statistically significant differences in the specific growth rate of duckweed *Lemna minor* except for pristine PE treatment where specific growth rate was significantly decreased in comparison to control (Fig. 5, Table S6). Similarly, no statistically significant differences were found when comparing the effects of microplastics on chlorophyll *a*. However, PE and UV-PE significantly affected root growth compared to control, but this was no longer observed after biodegradation (PE-BIO, UV-PE-BIO, Table S6). In addition, differences in the root lengths of duckweed in treatments with PE and UV-PE-BIO were also statistically significant (Table S6).

4. Discussion

Due to the global plastic crisis, numerous actions have been implemented to mitigate plastic pollution – the most important being the reduction of plastic waste through the widely adopted concepts of reduce, reuse, and recycle (Jia et al., 2019). However, these practices cannot be universally applied, as certain applications require the use of plastics. For example, agriculture relies on the use of plastic mulching films and a shift to the use of biodegradable alternatives such as PBAT has been observed over the previous two decades. Many studies showed that PBAT degrade well in the target environment, i.e., in soil or compost (Kijchavengkul et al., 2010; Liu et al., 2022), but some other studies showed that the degradation in soils is low (Han et al., 2021; Lee et al., 2024) or even reduced when PBAT is blended with other biodegradable polymers e.g. polylactic acid (PLA) (Palsikowski et al., 2018). Therefore, the actual biodegradation of PBAT in soil remains uncertain, and even less is known about their degradation in other, non-target environments.

The results of this study showed that the degradation in a non-target aquatic environment did not occur for pristine PE and UV-aged PE. Similarly, biodegradation of PBAT was low (Fig. 1), which is in agreement with the results of a study in which no degradation of pristine PBAT in lake sediments was observed over nine months (van Grinsven and Schubert, 2023) and similarly low degradation of PBAT was evaluated in the marine environment over six months (Lee et al., 2024). In general, lower degradation can be expected in the aquatic environment compared to the soil environment, which is linked to lower microbial activity and nutrient availability (Kaing et al., 2024). For example, our previous study showed fast degradation of chitosan plastic films (both with and without added antioxidants) in different soils (Oberlintner et al., 2021), while the same plastic films were only minimally degraded in the aquatic biodegradability test (Ročnik et al., 2020).

On the other hand, pre-exposure of PBAT to UV significantly enhanced its further degradation. FTIR analysis revealed a new absorption band appearing in the carbonyl region of PBAT spectra after UV-aging (inserted graph in Fig. 3B). Additional carbonyl groups are commonly reported in plastic and microplastics after UV-aging and indicate photodegradation (Alavian Petroody et al., 2023; Zidar et al., 2024). Therefore, it is plausible that UV-aging promoted the formation of carbonyl functional groups that are usually more easily utilized by microorganisms (Kotova et al., 2021). This would be also consistent with the biodegradation results, where the biodegradation of UV-PBAT increased 3.8-fold compared tothat of PBAT (Fig. 1). In addition, degradation was also visible by SEM as holes appeared on the surface of UV-PBAT after biodegradation (UV-PBAT-BIO, Fig. 2). Similarly, Convertino et al. (2024) also reported increased biodegradation of PBAT films in soil after UV-aging.

However, changes observed for PBAT following biodegradation may also be linked to the more rapid degradation of thermoplastic starch from the starch-PBAT blend, resulting in a relative enrichment of PBAT (Convertino et al., 2024; Pokhrel et al., 2021; Wang et al., 2015). This is relevant as many mulching film applications are expected to be exposed to UV radiation during use on the surface of field soils. But, in regions with low UV intensity, the degradation can be limited as the mulching films contain carbon black, which is used as a photostabiliser (Anunciado et al., 2021). They also contain other stabilisers and antioxidants to slow the degradation of the material (Hurley et al., 2024). Specifically, these additives can influence biodegradation either through leaching or by directly interacting while still being part of plastics. They can affect the diversity and activity of microbial community, potentially delaying biodegradation by extending the lag phase or reducing the biodegradation rate. However, microorganisms typically target the more accessible amorphous regions of the plastic, which are the first to degrade (Chan et al., 2025). As a result, the crystallinity tends to increase, as demonstrated in this study (Table 1). Notably, while the crystallinity of PE and PBAT remained relatively unchanged after UV irradiation (UV-PE and UV-PBAT), it significantly increased during the biodegradation experiment, but only for PBAT (PBAT-BIO and UV-PBAT-BIO). This suggests that microorganisms primarily utilized the carbon in amorphous regions, where it was better accessible (Mohanan et al., 2020). Additionally, it is plausible that PBAT underwent hydrolysis in the aquatic medium during the biodegradation experiment (Chan et al., 2025) as this process has been previously reported (Deshoulles et al., 2022). Monitoring changes in crystallinity is particularly important for low-density plastics, as an increase in crystallinity also leads to an increase in density, which in turn can affect the distribution of plastics in the aquatic environment (Budhiraja, 2024).

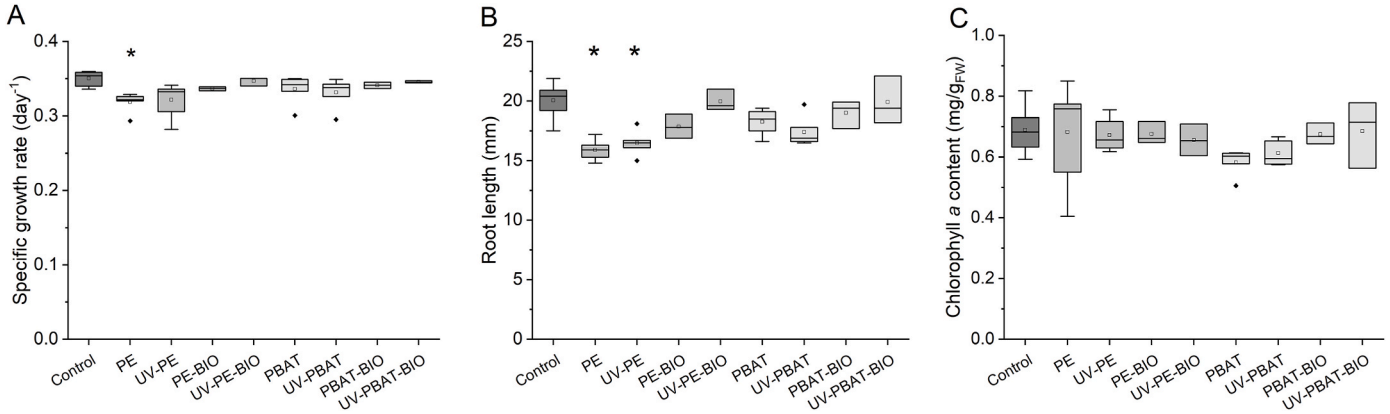

Fig. 5. The effects of pristine microplastics (PE, PBAT), after pre-exposure to UV (UV-PE, UV-PBAT) and after biodegradation (PE-BIO, PBAT-BIO, UV-PE-BIO, UV-PBAT-BIO) on (A) specific growth rate, (B) root growth, and (C) chlorophyll *a* content. * Significant difference compared to control ($p < 0.05$). Line – median, square – mean, box – 25–75 % of data, whiskers – range within 1.5 inter quartile range, deltoid - outlier.

However, further work is required to track the progress of degradation of PBAT and its constituent parts, and the corresponding impacts during this biodegradation process.

SEM analysis also revealed the presence of some microbial cells on the surface (Fig. 2), however, in a smaller amount compared to previous research, where PE fragments were aged in freshwater for 12 weeks (Rozman et al., 2023a). This is probably due to the very smooth surface of both PE and PBAT microplastics (Fig. 2) as it limits attachment of microorganisms (Rozman et al., 2023b). Agricultural mulch films contains many additives (Hurley et al., 2024) that may also affect biofilm development as they can act toxic limiting the growth of microorganism on the particles surface (Klun et al., 2023). If the biofilm cannot be developed on the plastic surface, the further degradation is likely to be limited (Debroy et al., 2022; Han et al., 2020).

Furthermore, LA-ICP-MS revealed alterations in some metals on the PE and PBAT surface. Metals within PE were stable, and the only alteration was in the case of Fe which accumulated on the surface of the microplastics. On the other hand, the lower content of Ti on PBAT after the biodegradation suggested leaching of Ti into the surrounding environment. Ti is often used as polycondensation catalysts in the production of PBAT so its presence can be expected (Jian et al., 2020). However, based on the amount of Ti in PBAT (Table S4) and taking into account concentration of PBAT in biodegradability and toxicity tests (100 mg/L), theoretical concentration of leached Ti (assuming complete leaching) would be 44.8 μg/L, which is not expected to affect aquatic organisms under test conditions (e.g. 168h EC_{50} of TiO_2 for duckweed is 539 mg/L (Kim et al., 2011)). Interestingly, PBAT contained also Pb but the reason or the origin of the Pb is unknown. It has to be noted that the use of highly sensitive LA-ICP-MS helped to reveal the presence of Pb despite the low content measured by to conventional method using acid digestion and liquid ICP-MS (Table S4).

Overall, the morphological, surface, and internal changes due to UV irradiation and exposure to microorganisms were minimal. Consequently, no significant changes were also observed in the ecotoxicity of PE and PBAT after biodegradation. In some cases, after biodegradation, the effects of PE were even lowered which is usually related to the smoothing of the microplastic surface due to the presence of some microbial cells (Jemec Kokalj et al., 2019), which was observed also when comparing PE and UV-PE-BIO treatments. However, further ecotoxicity studies using other aquatic species, like algae, crustaceans, and fish, would be needed to perform complete hazard assessment of biodegradable microplastics after environmental aging.

5. Conclusions

Plastics are used in our daily lives and in some cases their use cannot be avoided. Therefore, we need to find a sustainable way to deal with plastics or find alternatives that help to reduce plastic pollution and hazard in the environment. In this context, biodegradable plastics seem to be a good alternative, but their biodegradation must occur efficiently, fast, and with minimal impact on the environment. In this study microplastics derived from both conventional and biodegradable plastics prevalent in terrestrial environments were investigated, and we found that neither type exhibited biodegradability in non-target (aquatic) environments, as none met the required standards for classification as readily biodegradable material. Analytical techniques revealed that PE microplastics exhibited significant inertness, whereas some initial signs of degradation (mostly when microplastics were pretreated with UV) were observed through modifications in the FTIR spectrum and alterations in internal structure and morphology of PBAT microplastics. In the future, it would also be useful to combine conventional biodegradation tests with advanced analytical techniques when assessing the biodegradability of plastics, as these can provide important insights into the degradation and surface changes, the presence of a biofilm, the leaching of elements, changes in internal structure, and ecotoxicity. Together, they provide a comprehensive picture of the initial changes that plastics can undergo in the natural environment, their possible effects and their fate.

CRediT authorship contribution statement

Ula Putar: Writing – original draft, Validation, Methodology, Investigation, Formal analysis, Data curation, Conceptualization. **Aida Fazlić:** Writing – original draft, Formal analysis, Data curation. **Lukas Brunnbauer:** Writing – original draft, Investigation, Formal analysis, Data curation. **Janja Novak:** Writing – review & editing, Formal analysis, Data curation. **Anita Jemec Kokalj:** Writing – original draft, Validation, Supervision, Methodology, Conceptualization. **Jernej Imperl:** Writing – review & editing, Investigation, Formal analysis, Data curation. **Jiří Kučerík:** Writing – original draft, Validation, Supervision, Conceptualization. **Petra Procházková:** Writing – original draft, Formal analysis, Data curation. **Stefania Federici:** Writing – original draft, Validation, Methodology, Formal analysis. **Rachel Hurley:** Writing – review & editing, Investigation, Formal analysis. **Andrijana Sever Škapin:** Writing – review & editing, Methodology, Investigation, Formal analysis. **Pavlína Modlitbová:** Writing – review & editing, Validation, Supervision, Conceptualization. **Pavel Pořízka:** Writing – review & editing, Validation, Supervision, Methodology. **Jozef Kaiser:** Writing – review & editing, Supervision, Resources. **Andreas Limbeck:** Writing – original draft, Supervision, Resources, Methodology. **Gabriela Kalčíková:** Writing – original draft, Visualization, Supervision, Resources, Methodology, Funding acquisition, Conceptualization.

Declaration of competing interest

The authors declare that they have no known competing financial interests or personal relationships that could have appeared to influence the work reported in this paper.

Acknowledgements

The authors are thankful to Dr. Marija Zupančič for assistance with FTIR measurements and to Amadeja Sajovic Žulovec for her help with preparation of the biodegradability and toxicity test. This work was co-funded by the Slovenian Research and Innovation Agency (ARIS), the Czech Science Foundation (GAČR), and the Austrian Science Fund (FWF) under the *PLASTsensing* project (J1–4415, 23–13617L, I-6262-N, https://planterastics.fkkt.uni-lj.si), by Research programs P2–0191 and P2-0273 (ARIS), projects *PLAStouch* N2–0298 (ARIS), *μBioPlast* J1-50014 (ARIS), and PLAST-N-cycling (Z1-60166). The authors acknowledge the support of the Centre for Research Infrastructure at the University of Ljubljana, Faculty of Chemistry and Chemical Technology, which is part of the Network of Research and Infrastructural Centres UL (MRIC UL) and is financially supported by the Slovenian Research and Innovation Agency (Infrastructure programme No. I0-0022) and the support of the Faculty of Mechanical Engineering at the Brno University of Technology (no. FSI-S-23-8389). This article was also supported by the project "Mechanical Engineering of Biological and Bio-inspired Systems", funded as project No. CZ.02.01.01/00/22_008/0004634 by Programme Johannes Amos Commenius, call Excellent Research. The authors also thankfully acknowledge the support received from the Austrian Research Promotion Agency (FFG) in the frame of the Important Project of Common European Interest (IPCEI) on Microelectronics and Communication Technologies. The graphical abstract was created in BioRender.com. This article is based upon work from COST Action CA20101 Plastics monitoRIng detectiOn RemedIaTion recoverY - PRIORITY, supported by COST (European Cooperation in Science and Technology, www.cost.eu) and EU Horizon project PAPILLONS (g.a. 101000210).

Appendix A. Supplementary data

Supplementary data to this article can be found online at https://doi.org/10.1016/j.envpol.2025.126408.

Data availability statement

The data that support the findings of this study are openly available on Zenodo under the following link:https://doi.org/10.5281/zenodo.13884524.

References

Afshar, S.V., Boldrin, A., Astrup, T.F., Daugaard, A.E., Hartmann, N.B., 2024. Degradation of biodegradable plastics in waste management systems and the open environment: a critical review. J. Clean. Prod. 434, 140000. https://doi.org/10.1016/j.jclepro.2023.140000.

Alavian Petroody, S.S., Hashemi, S.H., Škrlep, L., Mušič, B., van Gestel, C.A.M., Sever Škapin, A., 2023. UV light causes structural changes in microplastics exposed in biosolids. Polymers 15 (21), 4322. https://doi.org/10.3390/polym15214322.

Anunciado, M.B., Hayes, D.G., Wadsworth, L.C., English, M.E., Schaeffer, S.M., Sintim, H. Y., Flury, M., 2021. Impact of agricultural weathering on physicochemical properties of biodegradable plastic mulch films: Comparison of two diverse climates over four successive years. J Polym Environ. Degrad. 29, 1–16. https://doi.org/10.1007/s10924-020-01853-1.

Boots, B., Green, D.S., Olah-Kovacs, B., De Falco, F., Lupo, E., 2023. Physical and chemical effects of conventional microplastic glitter versus alternative glitter particles on a freshwater plant (lemnaceae: lemna minor). Ecotoxicol. Environ. Saf. 263, 115291. https://doi.org/10.1016/j.ecoenv.2023.115291.

Briassoulis, D., Dejean, C., 2010. Critical review of norms and standards for biodegradable agricultural plastics part I. Biodegradation in soil. J. Polym. Environ. 18, 384–400. https://doi.org/10.1007/s10924-010-0168-1.

Brunnbauer, L., Jirku, M., Quarles, C.D., Limbeck, A., 2024. Capabilities of simultaneous 193 nm - LIBS/LA-ICP-MS imaging for microplastics characterization. Talanta 269, 125500. https://doi.org/10.1016/j.talanta.2023.125500.

Budhiraja, V., 2024. Degradation of Microplastics in the Environment. Doctoral Dissertation. University of Nova Gorica, Slovenia.

Cai, Y., Lv, J., Feng, J., 2013. Spectral characterization of four kinds of biodegradable plastics: poly (lactic acid), poly (Butylenes Adipate-Co-Terephthalate), poly (Hydroxybutyrate-Co-Hydroxyvalerate) and poly (Butylenes succinate) with FTIR and Raman spectroscopy. J. Polym. Environ. 21, 108–114. https://doi.org/10.1007/s10924-012-0534-2.

Chan, C.M., Serena, Y., Paul, L., Steven, P., Laycock, B., 2025. The impact of functional additives on biodegradable plastic biodegradation in natural terrestrial and composting environments. Crit. Rev. Environ. Sci. Technol. 55 (10), 708–731. https://doi.org/10.1080/10643389.2024.2443284.

Chen, X., Chen, C.-E., Guo, X., Sweetman, A.J., 2023. Sorption and desorption of bisphenols on commercial plastics and the effect of UV aging. Chemosphere 310, 136867. https://doi.org/10.1016/j.chemosphere.2022.136867.

Chen, X., Yue, Y., Wang, Z., Sun, J., Dong, S., 2024. Co-existing inorganic anions influenced the Norrish I and Norrish II type photoaging mechanism of biodegradable microplastics. Sci. Total Environ. 925, 171756. https://doi.org/10.1016/j.scitotenv.2024.171756.

Convertino, F., Carroccio, S.C., Cocca, M.C., Dattilo, S., Dell'Acqua, A.C., Gargiulo, L., Nizzetto, L., Riccobene, P.M., Schettini, E., Vox, G., Zannini, D., Cerruti, P., 2024. The fate of post-use biodegradable PBAT-based mulch films buried in agricultural soil. Sci. Total Environ. 948, 174697. https://doi.org/10.1016/j.scitotenv.2024.174697.

Crossman, J., Hurley, R.R., Futter, M., Nizzetto, L., 2020. Transfer and transport of microplastics from biosolids to agricultural soils and the wider environment. Sci. Total Environ. 724, 138334. https://doi.org/10.1016/j.scitotenv.2020.138334.

de Souza, A.G., Komatsu, L.G.H., Barbosa, R.F.S., Parra, D.F., Rosa, D.S., 2022. The effect of ZnO nanoparticles as Ag-carrier in PBAT for antimicrobial films. Polym. Bull. 79, 4031–4048. https://doi.org/10.1007/s00289-021-03681-2.

Debroy, A., George, N., Mukherjee, G., 2022. Role of biofilms in the degradation of microplastics in aquatic environments. J. Chem. Technol. Biotechnol. 97, 3271–3282. https://doi.org/10.1002/jctb.6978.

Deshoulles, Q., Gall, M.L., Benali, S., Raquez, J.M., Dreanno, C., Arhant, M., Priour, D., Cerantola, S., Stoclet, G., Gac, P.Y.L., 2022. Hydrolytic degradation of biodegradable poly(butylene adipate-co-terephthalate) (PBAT) - towards an understanding of microplastics fragmentation. Polym. Degrad. Stabil. 205, 110122. https://doi.org/10.1016/j.polymdegradstab.2022.110122.

Dilshad, E., Waheed, H., Ali, U., Amin, A., Ahmed, I., 2021. General structure and classification of bioplastics and biodegradable plastics. In: Kuddus, M., Roohi (Eds.), Bioplastics for Sustainable Development. Springer Singapore, Singapore, pp. 61–82. https://doi.org/10.1007/978-981-16-1823-9_2.

Gewert, B., Plassmann, M., Sandblom, O., MacLeod, M., 2018. Identification of chain scission products released to water by plastic exposed to ultraviolet light. Environ. Sci. Technol. Lett. 5, 272–276. https://doi.org/10.1021/acs.estlett.8b00119.

Ghaffar, I., Rashid, M., Akmal, M., Hussain, A., 2022. Plastics in the environment as potential threat to life: an overview. Environ. Sci. Pollut. Res. 29, 56928–56947. https://doi.org/10.1007/s11356-022-21542-x.

Griffin-LaHue, D., Ghimire, S., Yu, Y., Scheenstra, E.J., Miles, C.A., Flury, M., 2022. In-field degradation of soil-biodegradable plastic mulch films in a Mediterranean climate. Sci. Total Environ. 806, 150238. https://doi.org/10.1016/j.scitotenv.2021.150238.

Han, N., Zhao, Q., Ao, H., Hu, H., Wu, C., 2022. Horizontal transport of macro- and microplastics on soil surface by rainfall induced surface runoff as affected by vegetations. Sci. Total Environ. 831, 154989. https://doi.org/10.1016/j.scitotenv.2022.154989.

Han, Y., Teng, Y., Wang, X., Ren, W., Wang, X., Luo, Y., Zhang, H., Christie, P., 2021. Soil type driven change in microbial community affects poly(butylene adipate-co-terephthalate) degradation potential. Environ. Sci. Technol. 55, 4648–4657. https://doi.org/10.1021/acs.est.0c04850.

Han, Y.-N., Wei, M., Han, F., Fang, C., Wang, D., Zhong, Y.-J., Guo, C.-L., Shi, X.-Y., Xie, Z.-K., Li, F.-M., 2020. Greater biofilm formation and increased biodegradation of polyethylene film by a microbial consortium of arthrobacter sp. and streptomyces sp. Microorganisms 8 (12), 1979. https://doi.org/10.3390/microorganisms8121979.

Hoshino, A., Sawada, H., Yokota, M., Tsuji, M., Fukuda, K., Kimura, M., 2001. Influence of weather conditions and soil properties on degradation of biodegradable plastics in soil. J. Soil Sci. Plant Nutr. 47, 35–43. https://doi.org/10.1080/00380768.2001.10408366.

Hurley, R., Binda, G., Briassoulis, D., Carroccio, S.C., Cerruti, P., Convertino, F., Dvořáková, D., Kernchen, S., Laforsch, C., Löder, M.G.L., Pulkrabova, J., Schettini, E., Spanu, D., Tsagkaris, A.S., Vox, G., Nizzetto, L., 2024. Production and characterisation of environmentally relevant microplastic test materials derived from agricultural plastics. Sci. Total Environ. 946, 174325. https://doi.org/10.1016/j.scitotenv.2024.174325.

ISO, 2019. ISO 14851:2019 Determination of Ultimate Aerobic Biodegradability of Plastic Materials in an Aquaeous Medium - Method by Measurement the Oxygen Demand in a Closed Respirometer. ISO, Geneva, Switzerland.

Jemec Kokalj, A., Dolar, A., Nagode, A., Drobne, D., Kuljanin, A., Kalčíková, G., 2024. Response of terrestrial crustacean Porcellio scaber and mealworm Tenebrio molitor to non-degradable and biodegradable fossil-based mulching film microplastics. Sci. Total Environ. 951, 175379. https://doi.org/10.1016/j.scitotenv.2024.175379.

Jemec Kokalj, A., Horvat, P., Skalar, T., Kržan, A., 2018. Plastic bag and facial cleanser derived microplastic do not affect feeding behaviour and energy reserves of terrestrial isopods. Sci. Total Environ. 951, 175379. https://doi.org/10.1016/j.scitotenv.2017.10.020.

Jemec Kokalj, A., Kuehnel, D., Puntar, B., Žgajnar Gotvajn, A., Kalčikova, G., 2019. An exploratory ecotoxicity study of primary microplastics versus aged in natural waters and wastewaters. Environ. Pollut. 254, 112980. https://doi.org/10.1016/j.envpol.2019.112980.

Jia, L., Evans, S., Linden, S.v.d., 2019. Motivating actions to mitigate plastic pollution. Nat. Commun. 10, 4582. https://doi.org/10.1038/s41467-019-12666-9.

Jian, J., Xiangbin, Z., Xianbo, H., 2020. An overview on synthesis, properties and applications of poly(butylene-adipate-co-terephthalate)–PBAT. Adv. Ind. Eng. Polym. Res. 3, 19–26. https://doi.org/10.1016/j.aiepr.2020.01.001.

Kaing, V., Guo, Z., Sok, T., Kodikara, D., Breider, F., Yoshimura, C., 2024. Photodegradation of biodegradable plastics in aquatic environments: current understanding and challenges. Sci. Total Environ. 911, 168539. https://doi.org/10.1016/j.scitotenv.2023.168539.

Kalčíková, G., Žgajnar Gotvajn, A., Kladnik, A., Jemec, A., 2017. Impact of polyethylene microbeads on the floating freshwater plant duckweed Lemna minor. Environ. Pollut. 230, 1108–1115. https://doi.org/10.1016/j.envpol.2017.07.050.

Kijchavengkul, T., Auras, R., Rubino, M., Selke, S., Ngouajio, M., Fernandez, R.T., 2010. Biodegradation and hydrolysis rate of aliphatic aromatic polyester. Polym. Degrad. Stabil. 95, 2641–2647. https://doi.org/10.1016/j.polymdegradstab.2010.07.018.

Kim, E., Kim, S.-H., Kim, H.-C., Lee, S.G., Lee, S.J., Jeong, S.W., 2011. Growth inhibition of aquatic plant caused by silver and titanium oxide nanoparticles. Toxicol. Environ. Health Sci. 3, 1–6. https://doi.org/10.1007/s13530-011-0071-8.

Klun, B., Rozman, U., Kalčíková, G., 2023. Environmental aging and biodegradation of tire wear microplastics in the aquatic environment. J. Environ. Chem. Eng. 11, 110604. https://doi.org/10.1016/j.jece.2023.110604.

Kotova, I.B., Taktarova, Y.V., Tsavkelova, E.A., Egorova, M.A., Bubnov, I.A., Malakhova, D.V., Shirinkina, L.I., Sokolova, T.G., Bonch-Osmolovskaya, E.A., 2021. Microbial degradation of plastics and approaches to make it more efficient. Microbiology 90, 671–701. https://doi.org/10.1134/S0026261721060084.

Krimm, S., Liang, C.Y., Sutherland, G.B.B.M., 1956. Infrared spectra of high polymers. II. Polyethylene. J. Chem. Phys. 25, 549–562. https://doi.org/10.1063/1.1742963.

Lambert, S., Wagner, M., 2017. Environmental performance of bio-based and biodegradable plastics: the road ahead. Chem. Soc. Rev. 46, 6855–6871. https://doi.org/10.1039/c7cs00149e.

Lee, J., Kim, S., Park, S.B., Shin, M., Kim, S., Kim, M.-S., Shin, G., Kang, T., Kim, H.J., Oh, D.X., Park, J., 2024. Mimicking real-field degradation of biodegradable plastics in soil and marine environments: from product utility to end-of-life analysis. Polym. Test. 131, 108338. https://doi.org/10.1016/j.polymertesting.2024.108338.

Li, B., Liu, Q., Yao, Z., Ma, Z., Li, C., 2023. Mulch film: an overlooked diffuse source of organic ultraviolet absorbers in agricultural soil. Environ. Pollut. 318, 120935. https://doi.org/10.1016/j.envpol.2022.120935.

Liao, J., Chen, Q., 2021. Biodegradable plastics in the air and soil environment: low degradation rate and high microplastics formation. J. Hazard. Mater. 418, 126329. https://doi.org/10.1016/j.jhazmat.2021.126329.

Liu, Q., Wang, Y., Liu, J., Liu, X., Dong, Y., Huang, X., Zhen, Z., Lv, J., He, W., 2022. Degradability and properties of PBAT-based biodegradable Mulch films in field and their effects on cotton planting. Polymers 14 (15), 3157. https://doi.org/10.3390/polym14153157.

Mateos-Cárdenas, A., Scott, D.T., Seitmaganbetova, G., Frank, N.A.M.v.P., John, O.H., Marcel, A.K.J., 2019. Polyethylene microplastics adhere to Lemna minor (L.), yet have no effects on plant growth or feeding by Gammarus duebeni (Lillj.). Sci. Total Environ. 689, 413–421. https://doi.org/10.1016/j.scitotenv.2019.06.359.

Mazzon, M., Gioacchini, P., Montecchio, D., Rapisarda, S., Ciavatta, C., Marzadori, C., 2022. Biodegradable plastics: effects on functionality and fertility of two different soils. Appl. Soil Ecol. 169, 104216. https://doi.org/10.1016/j.apsoil.2021.104216.

Mohanan, N., Montazer, Z., Sharma, P.K., Levin, D.B., 2020. Microbial and enzymatic degradation of synthetic plastics. Front. Microbiol. 11. https://doi.org/10.3389/fmicb.2020.580709.

Moshood, T.D., Nawanir, G., Mahmud, F., Mohamad, F., Ahmad, M.H., AbdulGhani, A., 2022. Sustainability of biodegradable plastics: new problem or solution to solve the global plastic pollution? Curr. Opin. Green Sustainable Chem. 5, 100273. https://doi.org/10.1016/j.crgsc.2022.100273.

Napper, I.E., Thompson, R.C., 2023. Plastics and the environment. Annu. Rev. Environ. Resour. 48, 55–79. https://doi.org/10.1146/annurev-environ-112522-072642.

Niu, B., Chen, J.-B., Chen, J., Ji, X., Zhong, G.-J., Li, Z.-M., 2016. Crystallization of linear low density polyethylene on an in situ oriented isotactic polypropylene substrate manipulated by an extensional flow field. CrystEngComm 18, 77–91. https://doi.org/10.1039/C5CE01433F.

Oberlintner, A., Bajić, M., Kalčíková, G., Likozar, B., Novak, U., 2021. Biodegradability study of active chitosan biopolymer films enriched with Quercus polyphenol extract in different soil types. Environ. Technol. Innov. 21, 101318. https://doi.org/10.1016/j.eti.2020.101318.

OECD, 1992. Test No. 301: Ready Biodegradability, OECD Guidelines for the Testing of Chemicals, Section 3. OECD Publishing, Paris.

OECD, 2006. Test No. 221: lemna sp. growth inhibition test. OECD Guidelines for the Testing of Chemicals, Section 2. OECD publishing, Paris.

OECD, 2019. Test No. 203: Fish. Acute Toxicity Test.

Palsikowski, P.A., Kuchnier, C.N., Pinheiro, I.F., Morales, A.R., 2018. Biodegradation in soil of PLA/PBAT blends compatibilized with chain extender. J. Polym. Environ. 26, 330–341.

PhysicsOpenLab, 2022. Polymer anaylsis using Raman spectroscopy. https://physicsopenlab.org/2022/05/08/polymer-analysis-using-raman-spectroscopy/.

Pires, J.R., Souza, V.G., Fuciños, P., Pastrana, L., Fernando, A.L., 2022. Methodologies to assess the biodegradability of bio-based polymers—current knowledge and existing gaps. Polymers 14 (7), 1359. https://doi.org/10.3390/polym14071359.

Pischedda, A., Tosin, M., Degli-Innocenti, F., 2019. Biodegradation of plastics in soil: the effect of temperature. Polym. Degrad. Stabil. 170, 109017. https://doi.org/10.1016/j.polymdegradstab.2019.109017.

PlasticsEurope, 2024. Plastics - the Fast Facts 2023.

Pokhrel, S., Sigdel, A., Lach, R., Slouf, M., Sirc, J., Katiyar, V., Bhattarai, D.R., Adhikari, R., 2021. Starch-based biodegradable film with poly(butylene adipate-co-terephthalate): preparation, morphology, thermal and biodegradation properties. J. Macromol. Sci.,A 58, 610–621. https://doi.org/10.1080/10601325.2021.1920838.

Pořízka, P., Brunnbauer, L., Porkert, M., Rozman, U., Marolt, G., Holub, D., Kizovský, M., Benešová, M., Samek, O., Limbeck, A., Kaiser, J., Kalčíková, G., 2023. Laser-based techniques: novel tools for the identification and characterization of aged microplastics with developed biofilm. Chemosphere 313, 137373. https://doi.org/10.1016/j.chemosphere.2022.137373.

Ren, S.-Y., Kong, S.-F., Ni, H.-G., 2021. Contribution of mulch film to microplastics in agricultural soil and surface water in China. Environ. Pollut. 291, 118227. https://doi.org/10.1016/j.envpol.2021.118227.

Rosenboom, J.-G., Langer, R., Traverso, G., 2022. Bioplastics for a circular economy. Nat. Rev. Mater. 7, 117–137. https://doi.org/10.1038/s41578-021-00407-8.

Rozman, U., Filker, S., Kalčíková, G., 2023a. Monitoring of biofilm development and physico-chemical changes of floating microplastics at the air-water interface. Environ. Pollut. 322, 121157. https://doi.org/10.1016/j.envpol.2023.121157.

Rozman, U., Jemec Kokalj, A., Dolar, A., Drobne, D., Kalčíková, G., 2022. Long-term interactions between microplastics and floating macrophyte lemna minor: the potential for phytoremediation of microplastics in the aquatic environment. Sci. Total Environ. 831, 154866. https://doi.org/10.1016/j.scitotenv.2022.154866.

Rozman, U., Kalčíková, G., 2022. The response of duckweed Lemna minor to microplastics and its potential use as a bioindicator of microplastic pollution. Plants 11 (21), 2953. https://doi.org/10.3390/plants11212953.

Rozman, U., Klun, B., Kuljanin, A., Skalar, T., Kalčíková, G., 2023b. Insights into the shape-dependent effects of polyethylene microplastics on interactions with organisms, environmental aging, and adsorption properties. Sci. Rep. 13, 22147. https://doi.org/10.1038/s41598-023-49175-1.

Rozman, U., Turk, T., Skalar, T., Zupančič, M., Čelan Korošin, N., Marinšek, M., Olivero-Verbel, J., Kalčíková, G., 2021. An extensive characterization of various environmentally relevant microplastics – material properties, leaching and ecotoxicity testing. Sci. Total Environ. 773, 145576. https://doi.org/10.1016/j.scitotenv.2021.145576.

Ročnik, T., Oberlintner, A., Novak, U., Likozar, B., Kalčikova, G., 2020. The assessment of biodegradability of chitosan-based films. Book of Abstract. 26th Annual meeting of Slovenian Chemical Society, Portorož, Slovenia, pp. 16–18. September 2020.

Simul Bhuyan, M., S, V., S, S., Szabo, S., Maruf Hossain, M., Rashed-Un-Nabi, M., Cr, P., P, J.M., Shafiqul Islam, M., 2021. Plastics in marine ecosystem: a review of their sources and pollution conduits. Reg. Stud. Mar. Sci. 41, 101539. https://doi.org/10.1016/j.rsma.2020.101539.

van Grinsven, S., Schubert, C., 2023. Soil-biodegradable plastic films do not decompose in a lake sediment over 9 months of incubation. Biogeosciences 20, 4213–4220. https://doi.org/10.5194/bg-20-4213-2023.

Wang, H., Wei, D., Zheng, A., Xiao, H., 2015. Soil burial biodegradation of antimicrobial biodegradable PBAT films. Polym. Degrad. Stabil. 116, 14–22. https://doi.org/10.1016/j.polymdegradstab.2015.03.007.

Yang, Y., Li, Z., Yan, C., Chadwick, D., Jones, D.L., Liu, E., Liu, Q., Bai, R., He, W., 2022. Kinetics of microplastic generation from different types of mulch films in agricultural soil. Sci. Total Environ. 814, 152572. https://doi.org/10.1016/j.scitotenv.2021.152572.

Zidar, P., Kühnel, D., Škapin, A.S., Skalar, T., Drobne, D., Škrlep, L., Mušič, B., Jemec Kokalj, A., 2024. Comparing the effects of pristine and UV–VIS aged microplastics: behavioural response of model terrestrial and freshwater crustaceans. Ecotoxicol. Environ. Saf. 285, 117020. https://doi.org/10.1016/j.ecoenv.2024.117020.

Zong, X., Zhang, J., Zhu, J., Zhang, L., Jiang, L., Yin, Y., Guo, H., 2021. Effects of polystyrene microplastic on uptake and toxicity of copper and cadmium in hydroponic wheat seedlings (Triticum aestivum L.). Ecotoxicol. Environ. Saf. 217, 112217. https://doi.org/10.1016/j.ecoenv.2021.112217.